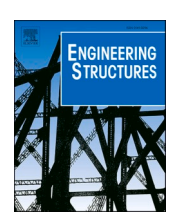
ELSEVIER

Contents lists available at ScienceDirect

Engineering Structures

journal homepage: www.elsevier.com/locate/engstruct





Evaluation of traffic load models for fatigue verification of European road bridges

Johan Maljaars

TNO, The Netherlands Eindhoven University of Technology, The Netherlands

ARTICLE INFO

Keywords:
Weigh in motion
Fatigue
Lorry
Heavy vehicle
Bridge
Load model

ABSTRACT

Fatigue verification of bridge structures requires information on the loads induced by heavy vehicles, which can be obtained from weigh in motion measurement (WIM) systems. The current fatigue load models applied in Europe are based on traffic load measurements in 1986. This paper evaluates the appropriateness of these models for today's traffic by comparing their load effects with those of recent WIM databases, covering the years 2008 to 2018. A procedure is derived to determine the required size of the WIM database for a sound representation of the fatigue loads. The effects of traffic jams are evaluated and the required safety margins or partial factors are derived. As already concluded by others, it appears that the most frequently used fatigue load model is unable to represent the fatigue action effects of today's European traffic. In addition, the paper demonstrates that the other fatigue load models are also inaccurate. A new fatigue load model is proposed that is easy in use and gives a significant improvement in accuracy compared to the existing models. The parameters in this model can easily be calibrated for other WIM databases.

1. Introduction

The European standard for actions on bridges, EN 1991-2 [1], provides fatigue traffic load models that should be used for the verification of fatigue of road bridges designed for Europe. Some of these models are intended to result into an unlimited fatigue life, whereas others are intended to provide a similar fatigue life as generated by the actual traffic. The models, briefly summarized in the appendix of this paper, should be used in combination with resistance models for fatigue, such as Wohler curves - also called S-N curves. The fatigue load models (FLMs) in [1] are calibrated using traffic load measurements - i.e. measurements of axle weights, vehicle composition and intervehicle distances of heavy vehicles - carried out in a motorway near Auxerre, France, in 1986, [2]. The traffic at Auxerre did not include the largest axle weights but it contained the highest frequency of large axle weights of the 25 motorways for which measured data were available at that time, [3], and it was therefore considered as one of the heaviest loaded locations in Europe. In addition, the recorded period was a number of weeks, which was substantial at that time.

The background of the calibration of the FLM-s is provided in [3,4,5]. Simulation software was developed that generates random 'traffic' arrays containing vehicles and the distance in between them. These arrays

were stepwise fed over an influence line and the load effect (such as bending moment) was recorded in time. A rainflow analysis was applied and the fatigue damage determined using an S-N curve that consists of a single slope. Each of the defined FLM-s was calibrated so as to obtain a stress range that would result in similar damage, or a stress range that remained below the constant amplitude fatigue limit. The 'traffic' arrays were generated from four standardized heavy vehicles with the distributions of axle weights, vehicle loads, and axle distance determined according to the measurements, see Fig. 1(a) for an example. It is unknown if and how the axle and load distributions of vehicles with a different configuration than the four mentioned vehicles are considered. The effects of dynamics were included by increasing the axle weights with a fixed value, that was based on a theoretical consideration. The intervehicle distances were generated from the recorded number of lorries per hour per lane, mean vehicle speed, the ratio between the number of heavy vehicles and other vehicles (cars and vans), and the fraction of lorries with a distance in between of less than 100 m to cover convoys. Flowing traffic has been considered only, because it was anticipated that traffic jams generally have a smaller contribution to the fatigue damage as compared to flowing traffic. Influence lines with a shape according to Fig. 1(b) were considered with various spans. The load models derived from the measurements were compared with traffic

E-mail address: johan.maljaars@tno.nl.

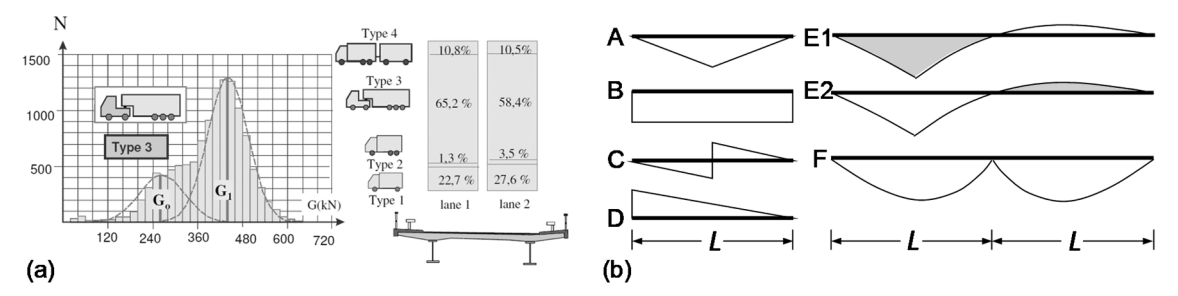


Fig. 1. Background of the derivation procedure of the FLM-s in EN 1991–2: (a) The four distinguished vehicle types and an example of the distribution definition (figure taken from [2]); (b) Shapes of the influence lines considered.

load measurements in other European motorways, e.g. [6,7].

The traffic composition, heavy vehicle construction, intervehicle distances, number of traffic jams, legislation and especially the number of heavy vehicles have changed since the measurements in 1986. The effects of such trends were not considered in the derivation and calibration of the FLM-s, [5]. In addition, the possibilities of measuring axle weights and vehicle compositions have increased. Weigh in Motion (WIM) systems are nowadays the standard for traffic load measurements and these allow for semi-permanent monitoring, [8].

Because of its wide usage in practice, most researchers evaluated the accuracy of FLM3 by comparing its load effect with that of more recent WIM databases. This model consists of two equal lorries that cross the influence line. The resulting stress ranges are multiplied with damage equivalent factors and then compared with the fatigue resistance, see the appendix. Simulation software was developed in Switzerland for evaluation purposes, [9], and it resulted that FLM3 was not able to accurately predict the fatigue damage for a large variety of influence lines, [10,11,12]. Modifications to the damage equivalent factors were proposed to better match the simulations. Simulations with traffic from other countries also demonstrated the poor performance of the load model, e.g. [13]. Leander [14] determined the reliability of FLM3, using a simulation in which single heavy vehicles passed the influence line, i.e. without other traffic being present on the influence line. The traffic data originated from BridgeWIM systems in Sweden. He showed a large variation of reliability index, β , between the influence lines considered, $0.9 < \beta < 4.9$, again demonstrating that the FLM is not calibrated for current European traffic. Summarizing the research carried out in the past, an extensive number of influence shapes has been studied, resulting in different damage equivalent factors for different shapes, e.g. [15,16], because one set of factors could not cover all influence lines. Research devoted to evaluate the accuracy of other FLM-s than FLM3 is

Most of the previous research used random (stochastic) simulations of traffic loads for evaluating the effects on the structure. The characteristics of actual traffic can, however, be very complicated and it is not straightforward to incorporate this in stochastic traffic simulations. Aspects that are difficult to model include the combination of vehicles on the outer lane (so called "slow lane") with overtaking vehicles on the adjacent lane ("fast lane") [17], the gradual development and dissolvement of traffic jams [16], the separation that is often experienced during rush hour traffic jams between heavy vehicles on the slow lane and passenger cars on the other lanes, and the inclusion of heavy vehicle types that are not frequent enough for an accurate fit with a distribution. One of the consequences is that almost all previous studies concerned influence lines loaded by a slow lane only. Some of the differences in the results of the previous studies can be attributed to differences in the random simulations. The return period of the load for verifications of the ultimate strength is so large that simulations are inevitable. For fatigue of road bridges, however, it has not been investigated what measurement period is required for an accurate representation of the load.

Instead of applying random simulations of traffic loads, this paper uses WIM data directly. A recent WIM database from the Dutch motorway A16 is used as a reference. The first part of the paper

evaluates this database on accuracy and consistency with other motorways. A method is developed to determine the size of the WIM database required for an accurate representation of the fatigue load. The second part compares the WIM database with the traffic load models. It proposes a new method for calibrating a simple FLM, which includes loading on multiple lanes. The emphasis of this paper is not so much on the results, but instead it is on the methods used to calibrate a FLM and to derive the required database size.

2. Description and representativeness of the WIM database

WIM measurements include the dynamic effects of vehicles because they are carried out with rolling vehicles. Given the ergodic character of these dynamic effects, even a relatively small database provides a realistic representation of rolling vehicles. The WIM databased considered is obtained from a WIM measurement station installed in the pavement of motorway A16 near Moerdijk in The Netherlands. The motorway consists of three continuous lanes per traffic direction. It is the main highway heading south or south east from the harbour of Rotterdam, which is one of the largest harbours in Europe. Periodic calibration of the WIM station is performed by measurement of vehicles with known axle weights. The WIM station is installed on the slow lane containing the majority of heavy vehicles, and the fast lane, containing vehicles that are overtaking vehicles on the slow lane. The third lane is forbidden for heavy vehicles and is therefore not measured. The WIM data of the months April in 2008, 2013 and 2018 have been considered. April is selected because it is a month with an average number of holidays in The Netherlands and the surrounding countries. The years 2008 and 2018 are characterized by economic booming whereas 2013 is a year of recession.

The annual number and summed weight of the heavy vehicles – defined as vehicles of which the total weight is at least 35 kN – are indicated in Table 1. The table indicates just a small change of number of heavy vehicles in the three years. Based on counting the number of vehicles on a large number of roads, the national road authority indicates that the maximum annual number of heavy vehicles is

Table 1 Numbers (#) and summed weights (Σ) of vehicles per traffic direction in the WIM database (and between brackets the ratio with the number and weights in 2008; grey cells).

year	2008	2013	2018
# lorries slow lane (x10 ³)	207 (1)	196 (0.95)	193 (0.93)
# lorries fast lane (x10 ³)	31 (0.15)	25 (0.12)	29 (0.14)
# 2-axles vehicles (x10 ³)	29 (0.14)	21 (0.1)	21 (0.1)
# 3-axles vehicles (x10 ³)	15 (0.07)	14 (0.07)	14 (0.07)
# 4-axles vehicles (x10 ³)	58 (0.28)	57 (0.28)	56 (0.27)
# 5-axles vehicles (x10 ³)	120 (0.58)	112 (0.54)	112 (0.54)
# 6-axles vehicles (x10 ³)	14 (0.07)	14 (0.07)	15 (0.07)
# 7-axles vehicles (x10 ³)	1 (0.01)	2 (0.01)	2 (0.01)
# greater than7-axles vehicles (x103)	1 (0)	1 (0)	1 (0.01)
Σ weight slow lane (x10 ⁶ kN)	48.7 (1)	42.1 (0.86)	50.8 (1.04)
Σ weight fast lane (x10 ⁶ kN)	6.9 (0.14)	5.6 (0.12)	6.4 (0.13)
# axles (x10 ³)	1036 (1)	985 (0.95)	984 (0.95)

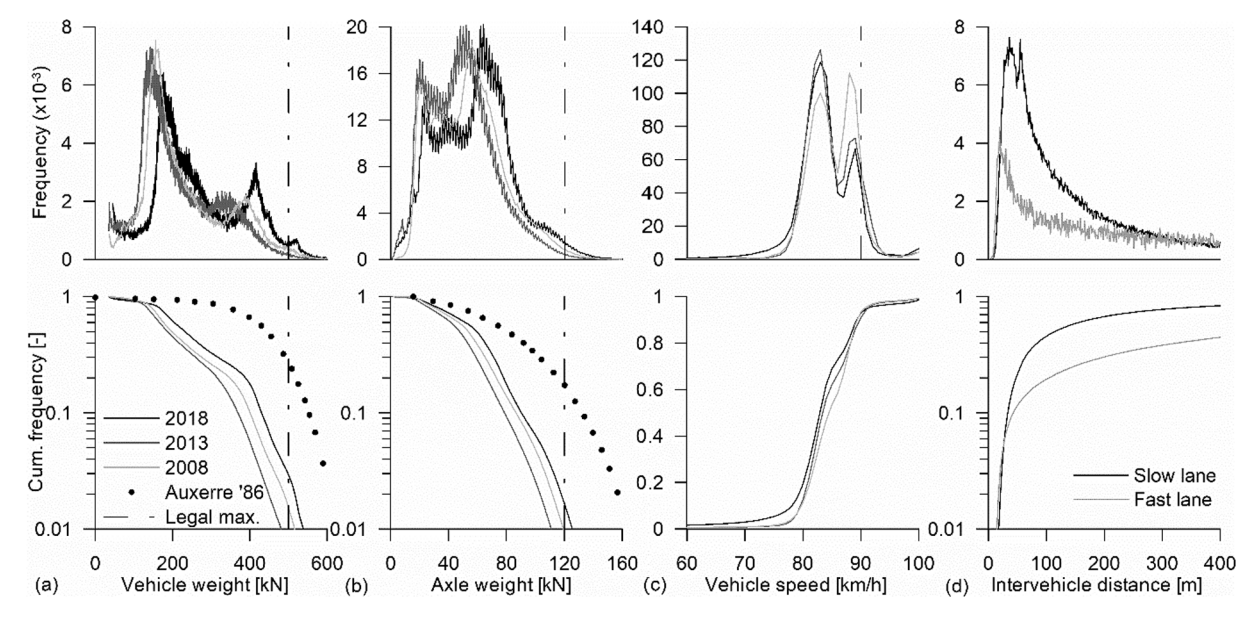


Fig. 2. Frequencies (top) and cumulative frequencies (bottom) of the A16 WIM databases: (a) Vehicle weight; (b) Axle weight; (c) Vehicle speed; (d) Intervehicle distances of the database from 2018.

approximately 2,5 million for a 3 lane road; the road is then "saturated" and a larger supply results into an increase in traffic jams. Comparing the numbers in Table 1 reveals that the motorway is saturated and this is believed to be the reason that the numbers are more or less constant over the years. The summed weights of the vehicles is lower in the recession year 2013 compared to the other two years. Fig. 2 provides the (cumulative) frequencies of the vehicle weights, axle weights, and vehicle speeds. The permitted maximum axle mass and vehicle mass in The Netherlands are 11500 kg and 50000 kg, respectively. Cranes are permitted with a mass up to 60000 kg. In addition, the authorities issue permissions for vehicle mass up to 100000 kg addressed to individual lorries. A small fraction of 2.5% of recorded axle weights exceeds the allowed static weight in 2018. This exceedance is attributed to differences in static and dynamic measurements and to overloading. Inaccuracies of the measurement system appear small, see the next section.

Comparing the WIM database to that of other European countries, it must be noted that legislation differs slightly between countries. This is a peculiar difference if one considers that freight transport is a highly international business, especially to and from the harbour of Rotterdam. The dashed curves of Fig. 2(a) and (b) provide the recorded weight distributions of the Auxerre database from 1986. The number of heavy vehicles per unit time that crossed the WIM station at Auxerre in 1986 is smaller than that of A16 in recent years. However, the plots indicate that the recorded Auxerre vehicles and axles are much heavier than those of the A16 in recent years. The vehicle and axle weights on A16 between 2018 correspond better to those of other motorways recorded around

1986 in [5]. A comparison between the A16 data and recent WIM database from other European motorways provides similar vehicle weights as for the Götthard traffic in Switzerland [18], motorway A2 in Spain [12], motorway 61 in Germany, motorway E17 in Belgium and motorway A23 in Austria (private communications), but higher weights as compared to motorway M4 in Ireland [19] and lower weights as compared to Swedish traffic in [14]. The Swedish traffic appears heavier than the Auxerre data from 1986. Note that the actual databases were not available to the author, so just the representation thereof in graphs and tables have been compared. The conclusions are that differences exist between motorways, that the A16 WIM database is in line with many other motorways in Europe, and that the Auxerre database from 1986 contains relatively heavy vehicles and axles, even when compared to today's traffic. To explain this latter aspect, Croce [12] suggests that the exceptional Auxerre traffic from 1986 may be caused by less accurate WIM systems that were available at that time.

The maximum permissible speed for freight transport depends on the vehicle type and is 80 km/h or 90 km/h for most heavy vehicles. Fig. 2 (c) indicates that the number of heavy vehicles involved in traffic jams — with low speed — is small. This is partially due to the small number of traffic jams at the recorded location and partially due to the small number of vehicles passing a certain location during a traffic jam. The intervehicle distances in Fig. 2(d), defined as the distance between the first axle of a heavy vehicle and the last axle of its predecessor in the same lane, not considering passenger cars, indicate that a significant number of heavy vehicles flows with a very short intervehicle distance.

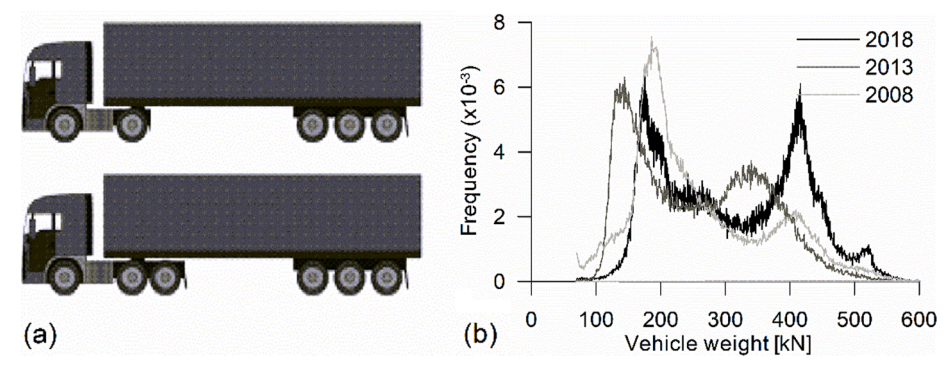


Fig. 3. Description and weight distribution of the "European lorry": (a) Configuration; (b) Relative frequency of the vehicle weight.

Indeed, the motorway has reached its maximum capacity during working hours; more vehicles are expected to cause more traffic jams and this may reduce the number of lorries that passes the station.

The fraction of so-called "European lorries", with 5 or 6 axles and a configuration according to Fig. 3(a), is 50–52% of the total number of heavy vehicles, where the 5 axle vehicles forms the largest fraction of the group. The fraction of the summed weight of the group in the total traffic is 58–62%. They are therefore the dominant vehicle type. Note that the actual percentage is even larger than measured because a certain number of 4 axle vehicles has one lifted rear axle and hence also belong to this type of vehicle. The relative frequency of the weight distribution of these lorries is indicated in Fig. 3(b). The figure indicates a wide distribution with two peaks, one describing empty lorries or lorries with relatively light weight freight, and one with relatively heavy freight. These two peaks are found for almost all vehicle types. The figure indicates that the vehicles were less loaded in the recession year 2013 and a larger number of relatively heavy vehicles is observed in 2018.

3. Accuracy and size of the WIM database

WIM systems installed in pavement require regular calibration by crossing of vehicles with known static axle weights and comparing these with the dynamic axle weights recorded by the WIM system. WIM systems are classified with respect to accuracy that is related to the calibration procedure. The WIM system investigated here is of accuracy class B, meaning a tolerance of 10% between the static and the WIM measured vehicle weight with a confidence interval of 90%, [8]. Calibration is typically carried out using a vehicle with known axle weights with magnitudes that occur frequently. The performance of the system in case of very heavy vehicles is thus subject to more uncertainty. In order to investigate the accuracy of the WIM database, its load effect is compared to strain gauge measurements on a bridge in another

motorway in The Netherlands that has similar vehicle characteristics.

The strain measurement location is the bottom flange of the main girder at 3/4 of the span of a double arch bridge with a total span of 354 m. The bridge has an orthotropic deck with asphalt pavement, two traffic directions and two lanes per traffic direction, but heavy vehicles are not allowed on the fast lanes, Fig. 4(a). The influence lines (Fig. 4(b)) are determined from a finite element model of the bridge, consisting of shell elements for the deck plate and beam elements for the arcs, main girders, crossbeams, bracings, hangers, and stringers of the orthotropic deck. Eccentric connections were applied between the elements to account for the distances between the beam neutral axes and the deck plate as well as the bearings. The influence line for lane 1 was checked by comparing the measured strains from a crossing vehicle with known static axle weights (Fig. 5(a)) with the stresses calculated using the influence line. The modulus of elasticity used to transfer the measured strains into stresses was $E = 206000 \text{ N/mm}^2$. The vehicle crossed the bridge four times, two times with a speed of 20 km/h and two times with 85 km/h. Fig. 5b provides the bridge response obtained from the strain measurements and calculated using the influence line. The figure shows a good agreement between the measured and calculated stresses. Some small peaks, indicated with arrows in Fig. 5b, are observed at the low speed crossings but not at the high speed crossings and in the calculations. These peaks are attributed to crossings of heavy vehicles in lane 4 during the tests. The high speed crossings show periodic stress variations with a frequency of 1.4 Hz and a magnitude of approximately 10% of the largest stress recorded after the vehicle has passed the strain gauge location. This demonstrates that the bridge is vibrating in its eigen mode. The largest range, however, is equal for the low and high speed crossings and is well captured with the model. The influence line is thus accurate.

Strains were also measured during three months in 2016 while the bridge was open for traffic. Six weeks in this period were free from holidays and road maintenance. These measurements were compared

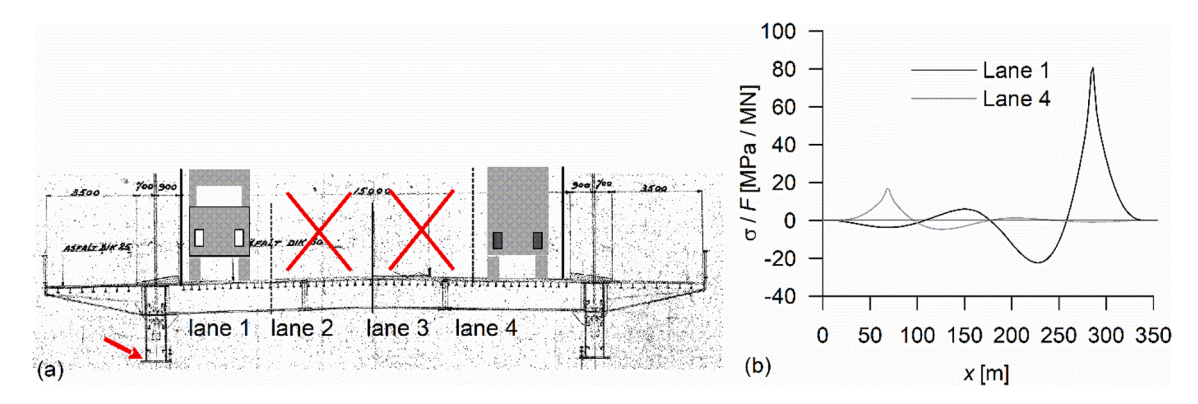


Fig. 4. Structural system of the bridge used to validate the WIM database: (a) Cross-section of the bridge, with strain gauge indicated by arrow; (b) Calculated influence lines.

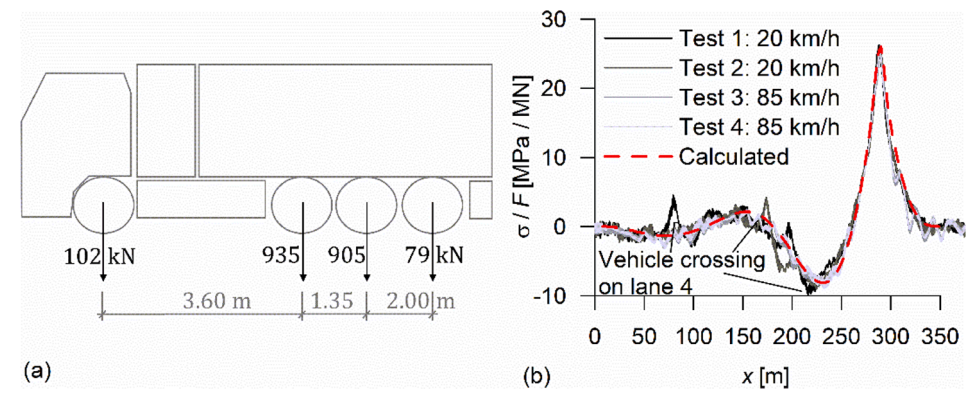


Fig. 5. Results of the influence line validation tests: (a) Configuration of the test vehicle; (b) Measured and calculated bridge response.

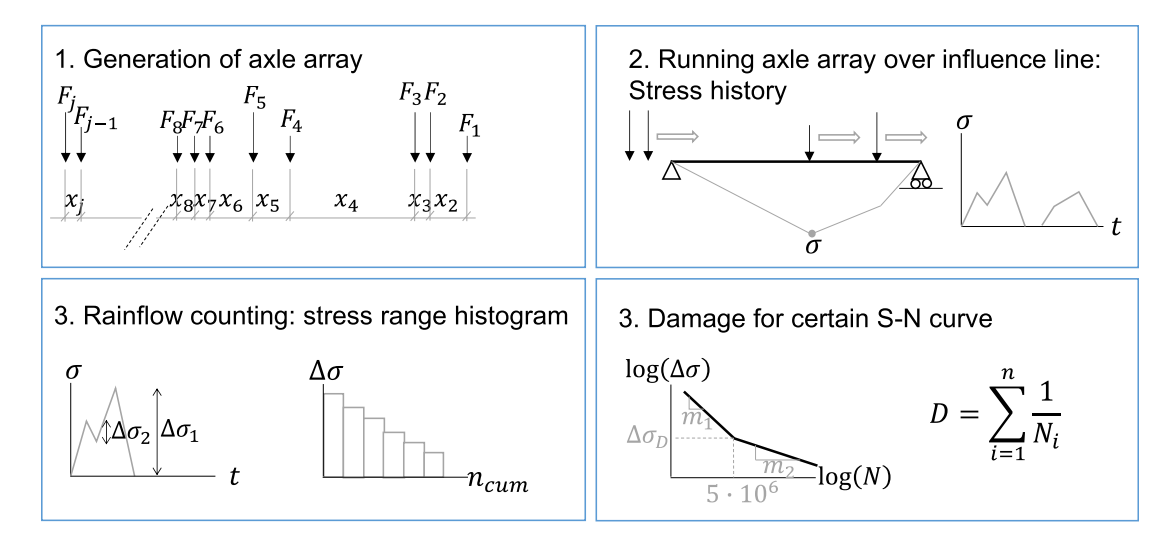


Fig. 6. Explanation of the simulation that determines the fatigue damage from an influence line and the WIM database.

with the calculated response using the influence lines and the WIM database. For this purpose, dedicated software is developed that runs the recorded axles over the influence lines of both traffic directions. Fig. 6 indicates the steps taken with the software: 1) It prepares a (thousands kilometres long) array of axles with their recorded weights and intermediate distances (considering distances between axles of each vehicle as well as between vehicles) according to the WIM database. 2) It runs this array over the influence line(s) of the respective lanes, considering slow and fast lanes and two traffic directions, and calculates the stress history. 3) It applies a rainflow counting procedure to provide the stress range histogram. 4) It calculates the theoretical fatigue damage, *D*, for a two-slope S-N curve together with the Palmgren-Miner damage accumulation rule:

$$D = \sum_{i=1}^{n} N_i^{-1} \tag{1}$$

$$N_i = 5 \cdot 10^6 \left(\frac{\Delta \sigma_D}{\Delta \sigma_i}\right)^{m_i} \tag{2}$$

$$m_i = \begin{cases} 3 & \text{if } \Delta \sigma_i \ge \Delta \sigma_D \\ 5 & \text{if } \Delta \sigma_i < \Delta \sigma_D \end{cases}$$
 (3)

where:

 N_i = number of cycles to failure for stress range $\Delta \sigma_i$.

 $\Delta\sigma_D=$ stress range of the knee-point of the S-N curve, assumed at $5\cdot10^6$ cycles in agreement with [20]. Its value depends on the type of detail considered.

 $m_i = \text{slope}$ parameter of the applicable part of the S-N curve.

n = number of applied cycles.

This resistance model is relatively simple; it corresponds with the common procedure used by practitioners to verify the fatigue resistance of structural details in bridges, [21].

The bridge vibration with magnitude of 10% of the largest stress recorded may influence the crossings of subsequent vehicles, but the overall increasing effect on the stress ranges is probably less than 10%, because not all vehicles are followed by others and because of the damping induced in case of multiple vehicles on the bridge. In order to take account of bridge vibration, the stress ranges in the histogram are therefore multiplied by dynamic amplification factors (DAF-s) with realistic values of 1, 1.03 and 1.05. The number of cycles are multiplied by the ratio between the number of vehicles recorded at the bridge and the number recorded in the motorway of the WIM system. A second simulation is performed using the WIM database of 2016 of the motorway in which the bridge is located, namely A27. Fig. 7(a) compares the stress range histograms obtained in this way with the measured histograms. The figure shows that the number of ranges with very low magnitude - 10 MPa or less - are underestimated using the procedure of Fig. 6. This is due to the fact that low weight vehicles are not included in the WIM database. This deviation is not important

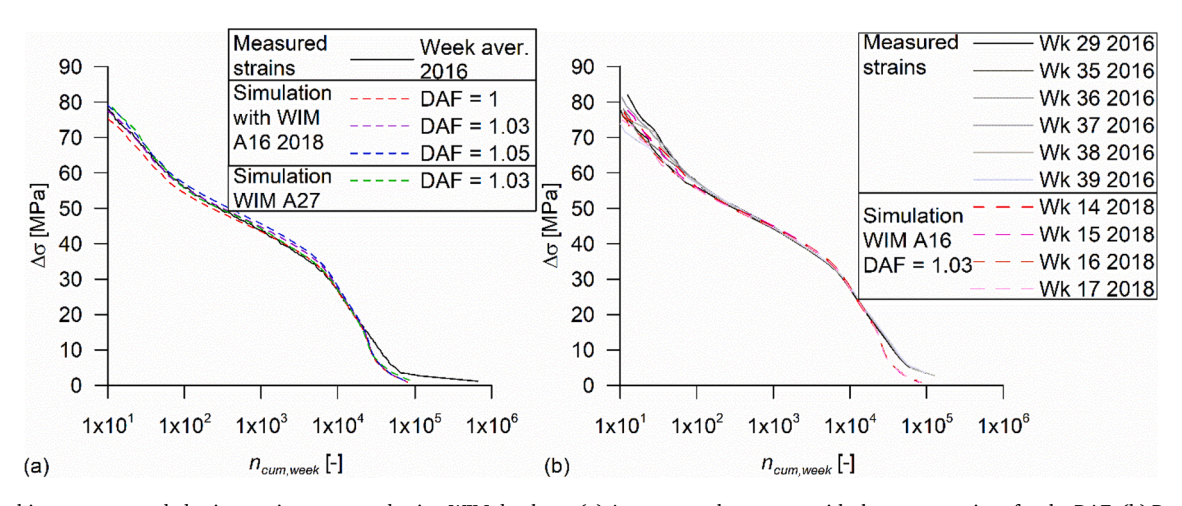


Fig. 7. Stress histograms recorded using strain gauges and using WIM database: (a) Average week response with three assumptions for the DAF; (b) Response of the individual weeks.

Table 2 Calculated weekly damage for $\Delta \sigma_D = 59$ MPa using strain gauge measurement and WIM database.

Measured strains	WIM,DAF=1	WIM, $DAF = 1.03$	WIM, $DAF = 1.05$
2.33 • 10-4	$2.06 \cdot 10^{-4}$	$2.38 \cdot 10^{-4}$	$2.61 \cdot 10^{-4}$

because the contribution to the fatigue damage of these ranges is negligible. A very good agreement is obtained between the measured and the calculated histograms for all stress ranges larger than 10 MPa. Table 2 gives the weekly fatigue damage D calculated for an S-N curve with a knee-point of $\Delta\sigma_D=59$ MPa. It also shows good agreement. Fig. 7 (b) provides the measured and calculated histograms per week. Both measurements and calculations show limited variation between weeks for the highest stress ranges only, with a comparable coefficient of variation. The good agreement between calculations and measurements demonstrates that the WIM database is sufficiently accurate for deriving FLM-s and that the software developed is sound. The good agreement between the measurement and the two WIM databases also indicates that the WIM database of A16 is representative for other motorways with similar traffic.

The return period required for the derivation of the extreme value of a traffic load effect to be used for ultimate strength verification is thousands of years. Hence, a stochastic model that represents traffic loads is adopted for ultimate strength verifications where the vehicle and axle mass distributions are based on WIM databases with a typical size of at least one month, e.g. [22], or statistical extrapolation models are applied using WIM databases with a size of one or several years, e.g. [23]. The return period for a representative fatigue loading is much lower. The author did not find a research into the representative return period of road traffic for fatigue verifications. A method is developed hereafter that allows to evaluate the required size of a WIM database for fatigue verifications. The theoretical fatigue damage is used as a reference for comparing the load effects relevant for fatigue. The influence lines considered in this section are representing influence lines of type A of Fig. 1(b) with spans of L = 5 m, 25 m and 100 m. The procedure of Fig. 6 is applied for each of these influence lines and the elastic section modulus, W_{el} , is determined in such a way that the fatigue damage after 1200 times running the WIM database over the influence line is equal to D=1, where 1200 is the number of months in 100 years, i.e. the structure is utilized to its maximum for a fatigue life of 100 years. This results into $W_{el}/\Delta\sigma_D = 55\cdot10^3$, $51\cdot10^4$, and $28\cdot10^5$ mm⁵/N for the spans of 5, 25 and 100 years, respectively. Subsequently, the database is divided into 30 databases of one day of traffic and the damage is determined for each day. Fig. 8(a) provides the damage per day, where a distinction is made between working days, Saturdays and Sundays (the two national holidays in April 2018 are ignored). The three spans give

an almost equal distribution of the daily damage. Normal and Student's t distributions are considered for the daily damages with average values and standard deviations as obtained from the data and the degrees of freedom based number of observations, Fig. 8(a). Using random drawings from these distribution functions and summing them per week, an artificial week damage is created. This is repeated 10⁴ times and the coefficient of variation of the damage, V_D , is determined from these 10⁴ realizations. Random drawings of the distribution functions representing daily damages were also summed for other periods, up to one year, and V_D is determined for each period. Fig. 8(b) provides the relationship between this period and V_D . As expected, the figure shows that V_D decreases with increasing period. For a period of 1 month, a very small damage variation of $V_D = 0.013$ (normal distributions) or 0.015 (Student's t distributions) results. Hence, a WIM database comprising one month of motorway traffic – equivalent to approximately 2:10⁵ vehicles - is certainly large enough for fatigue verifications.

An alternative method to verify the size of the database is also applied. In this method, the distances between vehicles is maintained as recorded in the WIM database but the vehicles with their axle weights and axle distances are randomly selected using the bootstrap method, i. e. with replacement of the vehicles. In this way, 10^3 databases are created and the damage is calculated for each database using the procedure of Fig. 6. The value of V_D of these 10^3 realizations is equal to 0.005. The small coefficient of variation again indicates that a WIM database constituting one month of motorway traffic is large enough for representing fatigue loads. Note that the period of one month does not contain variations over time, so-called trend effects. These are later in this paper accounted for.

4. Evaluation of intervehicle distances

Fig. 2 demonstrates that most vehicles are able to travel at almost full speed, but that the mode of the intervehicle distances is small. A similar distribution of the intervehicle distance was observed for the German motorway A7, [5]. This means that more than one vehicle load the influence line on a regular basis in case of spans larger than the vehicle length. More vehicles at the same time may imply a larger load effect and therefore more damage. On the other hand, in the extreme case a continuous loading causes only one load cycle and therefore short distances between vehicles may induce less damage as compared to individual vehicles. Leander [14] considered the load effect of each vehicle individually. In order to determine the influence between such an assumption and the actual database, simulations are carried out with type A influence lines of Fig. 1(b) with the complete WIM database including the recorded intervehicle distances, and with the individual vehicles in that same database but with intervehicle distances increased so that one vehicle passes the bridge at a time. The elastic section

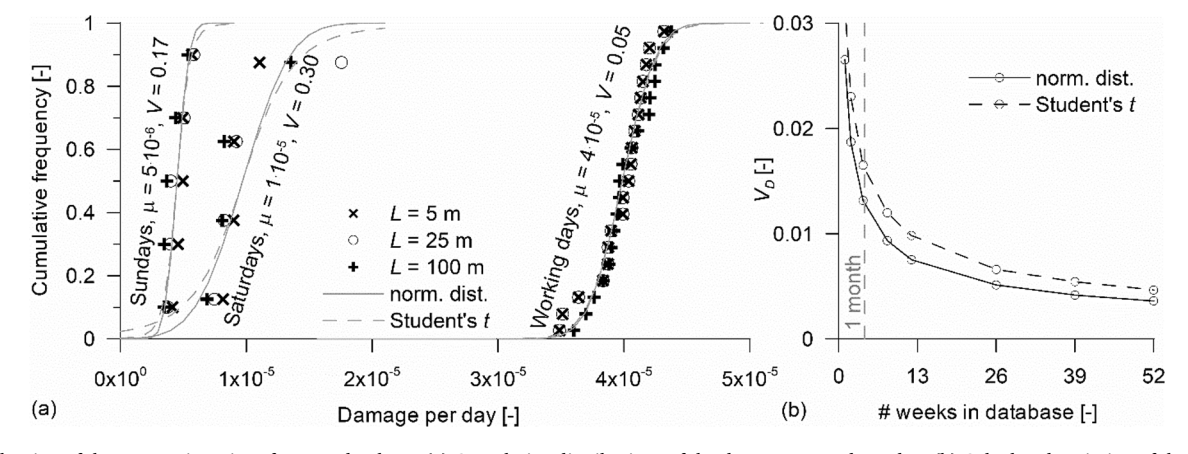


Fig. 8. Evaluation of the appropriate size of a WIM database: (a) Cumulative distributions of the damage created per day; (b) Calculated variation of the damage per database as a function of the database size.

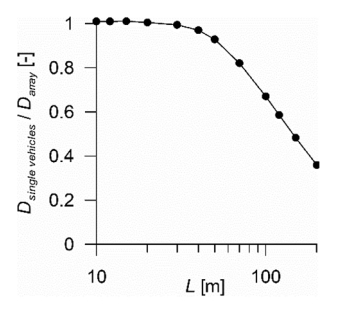


Fig. 9. Ratio of the summed damage of single vehicles and the damage of the entire WIM database for influence line type A.

moment was tuned for each span to arrive at a damage D=1 in 100 years, i.e. a structure completely utilized for fatigue. Fig. 9 provides the ratios between the damages of the individual vehicles and that of the WIM database. The figure demonstrates that the assumption of loading by individual vehicles makes no difference for spans $L \leq 30$ m and hardly any difference for 30 m $< L \leq 50$ m. For L > 50 m, the damage created by individual vehicles is smaller as compared to taking the recorded intervehicle distances into account. Loading by individual vehicles is too optimistic for dense traffic as recorded on motorway A16 and large spans. The same is valid for details loaded by more than one lane of any span.

The number and intensity of traffic jams vary between motorways. This may influence the fatigue damage contribution, because traffic jams influence the distance between vehicles and the number of vehicles per unit time that passes a bridge. The developers of the Eurocode FLM-s argue in [2] that flowing traffic produces more damage than traffic jams, because of a smaller number of vehicles passing the bridge in a traffic jam and because more vehicles loading the influence line at the same time may interfere their dynamical effect, thereby reducing the total dynamic amplification. On the contrary, [15] predict a larger load effect and hence more fatigue damage for congested traffic as compared to flowing traffic on the basis of simulations. This section evaluates the effect of traffic jams on the fatigue damage based on the recent A16 WIM database.

Motorway A16 has regular traffic jams a few kilometres north and south of the WIM station during morning and evening rush hours on working days. Congestion at the location of the WIM station itself is, however, low. The traffic speed distributions of Fig. 2(c) demonstrate that the database of 2018 contains some more congestion as compared to the databases of 2008 and 2013. In order to determine the influence of congestion on the fatigue damage, two working days from the 2018 database are compared. A certain time window is selected for which the speed of the individual vehicles showed clear signs of a traffic jam (black

dots in Fig. 10(a)). The same time window of the day before was selected and showed no traffic jam (grey dots). An accident or construction works was the probable cause of the traffic jam, considering the hours of the window. The reason to select this traffic jam - and not a rush hour traffic jam – was that it provides a clear distinction between the two subsequent days. The time window of the day with jam was subdivided into two windows, namely w_1 in which the traffic jam developed and dissolved and w_2 that showed the pulsating effect characteristic to a fully developed traffic jam. This subdivision is made because the duration of fully developed traffic jams w_2 varies, but w_1 is expected being more constant. The average damage rates of these two time windows, i.e. the calculated damage increase per minute \dot{D}_{w1} and \dot{D}_{w2} averaged over all minutes in the time windows, are determined with the procedure of Fig. 6 and compared with the damage rate of the flowing traffic of the previous day, \dot{D}_{flow} . This is done for the type A influence line of Fig. 1(b) loaded by the slow lane only, with spans $10 \text{m} \leq L \leq 100 \text{m}$. Fig. 10 (b) gives the ratios between the damage rates of the traffic jam situations and that of the flowing traffic. The figure shows that the damage rate of window w_2 is smaller than that of flowing traffic. This is mainly due to the smaller number of vehicles per unit time that passes the slow lane in window w_2 (ratio 0.91 with flowing traffic, against ratio 1.06 for w_1 versus flowing traffic). Fig. 10(c) gives the average damage contribution per vehicle, ΔD . One would not expect any influence of congestion on the average damage per vehicle for short spans of e.g. 10 m – i.e. $\Delta D_{jam}/\Delta D_{flow}=1 \text{ in Fig. } 10(c)$ – because the load effect is not depending on the intervehicle distance for short span. The small deviation from unit at short spans is attributed to random differences in average vehicle weights of the windows. Additional to this difference, Fig. 10 demonstrates that the ratios between the damage rates and damage per vehicle decrease with increasing span. This is attributed to the smaller distances between the vehicles in a traffic jam as compared to flowing traffic, resulting in more continuous loading and hence a smaller number of ranges for longer spans.

This evaluation concerned one traffic jam only, hence one must be careful in generalizing these results. On the other hand, the coefficient of variation of the damages per working day is small: $V=0.05({\rm Section~3})$, hence it is unlikely that very different observations will follow in case of other traffic jams. Evaluating the damages generated by all individual days for spans of 5, 25 and 100 m and considering the amount of congestion of these days (the latter estimated based on the traffic speed), no significant correlation was found between these two aspects. Hence, congestion is expected to have no or only a slightly positive contribution to the fatigue life as compared to the flowing, dense traffic recorded on motorway A16. The difference in conclusion of [15], which predicted a negative influence of traffic jams, is expected to relate to the less compact flowing traffic in that study, with 1/5 of the number of vehicles recorded on motorway A16.

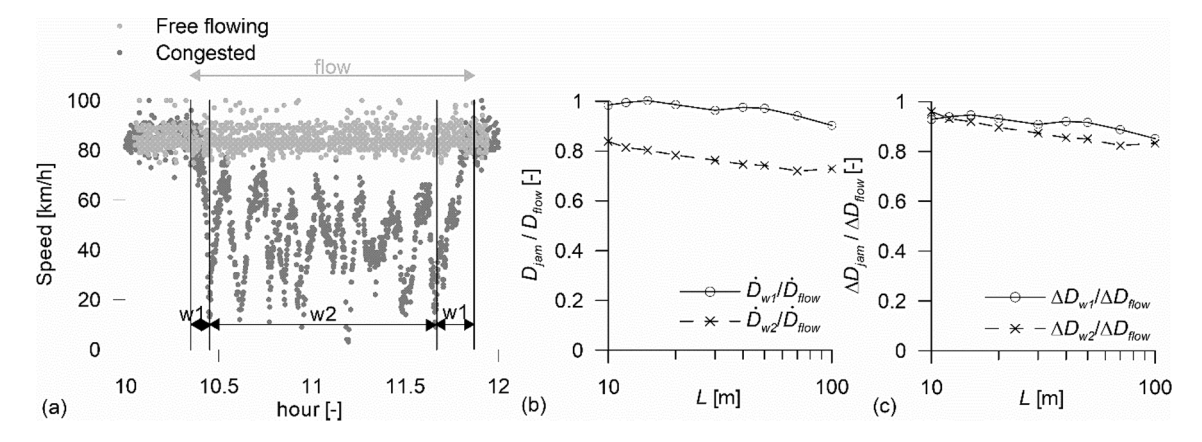


Fig. 10. Evaluation of the influence of a traffic jam on the damage: (a) Speed of individual heavy vehicles, and definition of time windows w_1 , w_2 , and flow; (b) Comparison of the damage rates; (c) Comparison of the average damage per heavy vehicle.

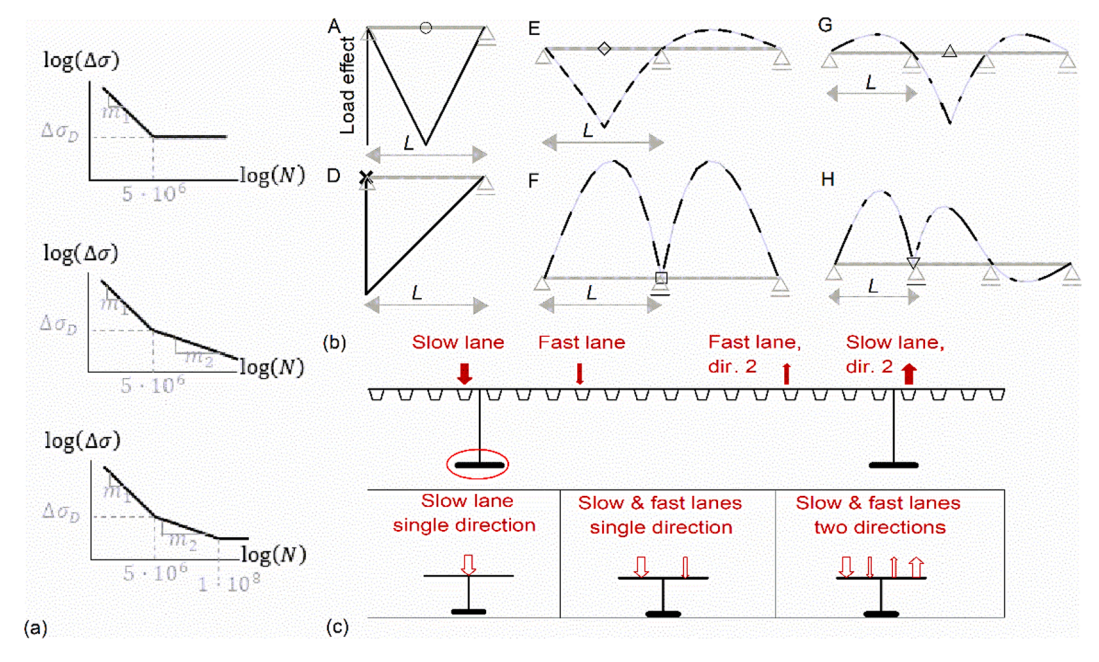


Fig. 11. Cases considered in determining the accuracy of the FLM-s: (a) S-N curves; (b) Influence lines; (c) Number of lanes and traffic directions.

5. Accuracy of the fatigue load models in the Eurocode

Now that the database and the procedure are validated, they are used to determine the accuracy of the FLM-s in EN 1991–2 [1]. The appendix of this paper describes these FLM-s. FLM1 and 2 are intended to design for infinite life, FLM3 and 4 to design for sufficient life, i.e. $D \leq 1$. It should be noted that none of the FLM-s is intended to (accurately) represent the actual traffic. Instead, they are intended to obtain a similar load effect relevant to fatigue, as the actual traffic, either by providing a maximum load (FLM1 and 2), an equivalent load (FLM3) or similar damage (FLM4).

Fig. 11 summarises all cases that are considered for determining the accuracy of the FLM-s. A one-slope S-N curve with a constant amplitude fatigue limit (CAFL) at $\Delta\sigma_D$ is used for FLM1 and 2 (top graph of Fig. 11 (a)) and the two-slope S-N curve for FLM3 and 4 (centre graph of Fig. 11 (a)). A variant of the two-slope S-N curve is also considered, containing a cut-off limit at 10^8 cycles. This variant, shown at the bottom of Fig. 11(a) corresponds with the Eurocode S-N curve definition, [20]. The influence lines considered are the most relevant ones from the former calibration, Fig. 1(b), and in addition three-span cases, see Fig. 11(b). Most other influence lines for practical cases have a shape that is similar to one of

the lines considered here. The spans considered for each influence line range between 1 m \leq $L \leq$ 200 m. In a realistic bridge configuration, the structural components are usually loaded by a combination of traffic lanes with different magnitudes of the influence lines, see the top graph of Fig. 11(c). This study considered three extreme cases according to the bottom graphs of Fig. 11(c): a component loaded by a slow lane only, a component loaded by the slow and fast lane of one traffic direction, with equal influence lines; and a component loaded by four lanes, two traffic directions, all having equal influence lines. The influence lines of a component in an actual bridge are in most cases bounded by these extreme cases. For all of these cases, the elastic section modulus that is designed using the WIM database, $W_{el,WIM}$, is determined using the procedure of Fig. 6, as well as the elastic section modulus designed using the FLM, $W_{el.FLM}$. The WIM database, comprising one month of traffic, is applied 1200 times to reflect a fatigue life of 100 years. The ratio $\frac{W_{elFLM}}{W_{elWM}}$ is used as an indicator for the accuracy of the FLM. (Load model uncertainties are considered in the next section.)

Using FLM1 and 2, the elastic section modulus $W_{el,FLM}$ is designed in such a way that "infinite life" is obtained. The maximum stress ranges determined with these models should for this purpose be equal to (or

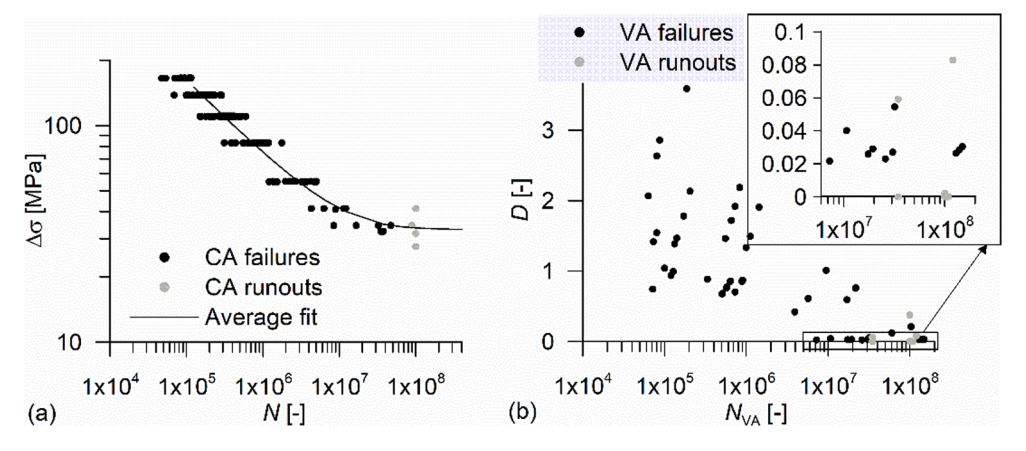


Fig. 12. Analysis of tests on full scale welded cover plates: (a) CA test data and average regression curve using a random fatigue limit model; (b) VA test data versus damage calculated with the average regression curve for CA data.

Fig. 13. Ratios $\frac{W_{d,FLM}}{W_{d,WIM}}$ for FLM 1 and 2, considering a non-propagating crack: (a) Single slow lane; (b) Slow and fast lanes, 1 direction; (c) Slow and fast lanes, 2 directions.

smaller than) $\Delta \sigma_D$. However, in any stochastic load process, there is always a probability that a certain stress range is exceeded. Moreover, there is no consensus about the existence of a constant amplitude fatigue limit, [30,31]. For these reasons, the elastic section modulus is determined using the WIM database and the procedure of Fig. 6, in such a way that a non-propagating crack results. This condition is assumed if the damage using the constant-amplitude S-N curve of Fig. 11(a), D_{CA} , is equal to (or smaller than) a critical value, D_{lim} . The value of D_{lim} must thus be selected. According to [32], a propagating crack may already occur if the number of stress ranges above the CAFL is 0.01% of the total number of ranges. This conclusion was based on tests in [33]. Using the same test data plus test data from additional sources [34,35], an updated criterion for a non-propagating crack is derived here. All data consider full scale welded cover plate joints. A best fitted S-N curve is determined using the constant amplitude (CA) fatigue test data and a random fatigue limit model in [36], see Fig. 12(a). Variable amplitude (VA) test data were carried out with Rayleigh stress range spectra, in some cases with additional large cycles above the CAFL. Fig. 12(b) provides the number of cycles to failure of the VA test data together with the damage determined using the best fitted CA S-N curve. The figure demonstrates that all but three VA tests failed when the damage produced with the CA S-N curve is $D_{CA} \ge 0.02$. Based on this evaluation, the criterion used for a non-propagating crack is $D_{lim} = 0.02$.

The accuracy of FLM1 and 2 is now determined. As an example, a type A influence line of Fig. 1(b) with a span of L=50 m loaded by a slow lane with a width of 3 m gives a maximum bending moment at midspan of 7.66 MNm or 6.80 MNm when designed with FLM1 or FLM2, respectively. The maximum bending moment resulting from the WIM database in the month considered is 12.51 MNm, i.e. much larger than the maximum values according to the FLM-s. Using an S-N curve with $\Delta\sigma_D=66$ MPa the required elastic section modulus is 0.12 m³ or 0.10 m³ for FLM1 or FLM2, respectively, whereas the criterion $D_{CA}=D_{lim}$ using the WIM database and a design life of 100 years requires an elastic section modulus of 0.14 m³, i.e. still larger than according to the FLM-s.

Fig. 13 gives the ratio between W_{el} determined with FLM1 and FLM2, $W_{el,FLM}$, and the section modulus required for a non-propagating crack $(D_{CA} = D_{lim})$ with the WIM database, $W_{el,WIM}$. For influence line type D, this ratio is to be considered as the shear area ratio. The line shapes and symbols refer to the corresponding shapes and symbols in Fig. 11(b). FLM2 is not considered for loading by multiple lanes nor for large spans, because its application area is limited to situations where the presence of simultaneous vehicles on the influence line can be ignored, [1]. Following Fig. 9, this is the case for L < 50 m. The figure demonstrates that W_{el} determined with FLM2 for loading by a slow lane is lower than that required with the WIM database – i.e. FLM2 is too optimistic, or is at least not providing infinite life – for spans exceeding 5 m. The same applies to FLM1 for spans between 12 and 120 m loaded by a slow lane only. With respect to FLM1 it is important to note that the component is loaded by a slow lane only; if an escape lane or another non-regular loaded part of the bridge loads the detail in addition to the slow lane, $W_{el,FLM}$ for FLM1 will increase but $W_{el,WIM}$ and $W_{el,FLM}$ for FLM2 remain unaltered. Hence the conclusion on the safety of FLM1 may change in that case. For components loaded by multiple lanes, the figure indicates that FLM1 requires a larger elastic section modulus than the WIM database for most cases considered. However, a large dependency exists between the span and the level of conservatism.

The ratio between W_{el} designed with FLM3 and 4 and W_{el} using the WIM database is determined for a life of 100 years. Fig. 14 provides the results. The figure demonstrates that the load models lack accuracy. FLM3 requires a smaller elastic section modulus than the actual traffic (WIM database) for a number of cases but a larger elastic section modulus in other cases. FLM3 is bounded to spans of 80 m in EN 1991–2. In addition, according to the background document [3], FLM3 is derived for spans larger than 20 m but this limitation is not provided in EN 1991–2. The scatter of FLM4 for different influence lines is smaller than that of FLM3, but the amount of conservatism of FLM4 depends on the span length. Application rules for FLM4 are lacking for two traffic directions, therefore Fig. 14 does not show this case.

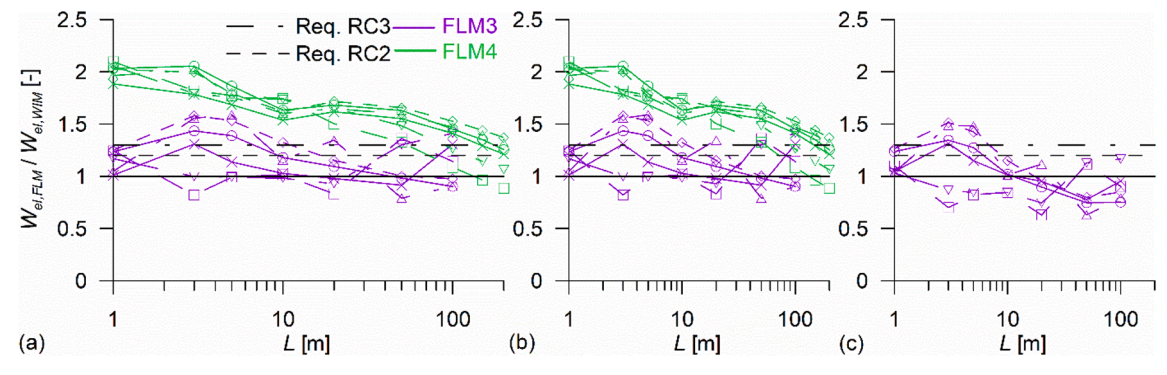


Fig. 14. Ratios $\frac{W_{distrat}}{V_{distrat}}$ for FLM 3 and 4 and a design life of 100 years: (a) Single slow lane; (b) Slow and fast lanes, 1 direction; (c) Slow and fast lanes, 2 directions.

6. Structural reliability and partial factors

The load effect and the resistance are subject to epistemic and aleatory uncertainties. A simplified probabilistic analysis is conducted to determine the reliability of a structural design using the FLM-s described above. A first step in such an analysis is describing the uncertainties. First, the structural model of the bridge component may deviate from the actual behaviour e.g. due to simplifications applied by the engineer. The influence line is thus subject to uncertainty. Following the recommendation in in [24], a lognormal distributed stress range multiplier with an average value of $\mu_{Uf}=1$ and a standard deviation of $s_{Uf}=0.1$ is considered to account for this uncertainty.

Second, a WIM system installed in pavement includes the dynamic effects of rolling vehicles but does not contain dynamic effects caused by interaction between vehicles and the bridge structure. These dynamic effects depend on resonance frequencies, damping values, and masses of vehicles and the bridge. A large number of studies is devoted to estimating dynamic effects, where [25] and [26] are interesting because of the combination of dynamic simulations and statistical analysis of data. However, existing studies are devoted to extreme value estimates of load effects for ultimate strength verification. The dynamic effects for fatigue are expected to be lower than that, because of the fact that fatigue relates to the cumulative damage created by many vehicles with a statistical distribution of the dynamics per vehicle. Measurements carried out at several bridge structures in The Netherlands show a small or even negligible dynamic amplification, irrespective of the length of the influence line. A lognormal distributed stress range multiplier with an average value of $s_{Ud} = 1$ and a standard deviation of $s_{Ud} = 0.05$ is therefore considered in this study for these dynamic effects.

Third, axle and vehicle weights and numbers of vehicle may change in time. Since the period of the first records of traffic loads, around 1950, the numbers and weights have increased but measurements of more recent date do not show a distinct weight increase. Table 1 indicates a small difference between the recorded databases in the period between 2008 and 2018. However, bridges are typically designed for a 100 year life and it is almost impossible to predict trends in traffic over such a long future period. The trends depend to a large extend on (inter)national legislation e.g. with respect to the allowance of automatic vehicle driving and platooning. The reasoning is followed here that, once legislation changes, a new situation is created that requires recalibration of load models as well as re-assessment of existing structures. These aspects are therefore not considered in the current study. Remaining is the uncertainty in trends without legislation changes, for which a lognormal distributed stress range multiplier with an average value of $\mu_{Ut}=1.0$ and a standard deviation of $s_{Ut}=0.05$ is assumed here. The combined load effect multiplication factor that considers the uncertainty has thus an average value of $\mu_U = \mu_{U\!f} \cdot \mu_{U\!d} \cdot \mu_{Ut} = 1.0$ and a standard deviation of approximately $s_U \approx \sqrt{s_{Uf}^2 + s_{Ud}^2 + s_{Ut}^2} = 0.12$.

Characteristic S-N curves in EN 1993-1-9 [20] are defined with a one-sided 95% lower prediction bound, [27]. Assuming the S-N curves are based on a large number of tests, so that the epistemic uncertainty is negligible as compared to the aleatory uncertainty, only the latter needs to be defined. Representing the aleatory uncertainty in absence of actual data, [28] provides a standard deviation of the 10-base logarithm of the number of cycles to failure $s_{SN}=0.2$. The difference between the characteristic and the average S-N curve is thus $\mu_{SN}=1.645 \cdot s_{SN}=0.33$. In agreement with [24] and [28] the two branches of the S-N curve are fully correlated, see Fig. 15. In addition, these guidelines consider uncertainty in the damage summation of Palmgren Miner by specifying a critical damage variable with a lognormal distribution with mean of $\mu_D=1.0$ and standard deviation $s_D=0.3$. Table 3 gives an overview of the random variables.

The limit state function is defined as:

$$g(X) = X_D - D_n \tag{4}$$

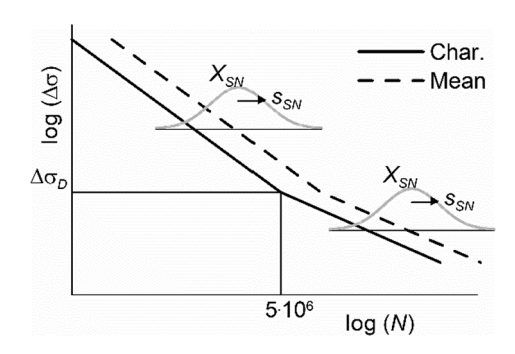


Fig. 15. Probabilistic S-N curve with full correlation between the two branches.

Table 3
Random variables.

X	Description	Distribution type	Mean [-]	Stand. dev. [-]
X_U	Combined uncertainty on the load effect	lognormal	1.0	0.12
X_{SN}	Scatter of $log_{10}(N)$ in the S-N curve	normal	0.33	0.2
X_D	Uncertainty Miner sum	lognormal	1.0	0.3

where

$$D_n = \frac{1}{5 \cdot 10^{(6 + X_{SW})}} \sum_{i=1}^n \min \left[\left(\frac{X_U \cdot \Delta \sigma_i}{\Delta \sigma_D} \right)^3, \left(\frac{X_U \cdot \Delta \sigma_i}{\Delta \sigma_D} \right)^5 \right]$$
 (5)

The structural design is made using the characteristic S-N curve and the partial (safety) factors on the resistance side, γ_{Mfat} , and on the load side, γ_{Ffat} . The design value of the damage is:

$$D_{d} = \frac{1}{5 \cdot 10^{6}} \sum_{i=1}^{n} \min \left[\left(\frac{\gamma_{Mfat} \cdot \gamma_{Ffat} \cdot \Delta \sigma_{i}}{\Delta \sigma_{D}} \right)^{3}, \left(\frac{\gamma_{Mfat} \cdot \gamma_{Ffat} \cdot \Delta \sigma_{i}}{\Delta \sigma_{D}} \right)^{5} \right]$$
 (6)

Note that Eq. (6) is the same as the combination of Eqs. (1–3), but it includes the partial factors. For several combination values of γ_{Mfat} , γ_{Ffat} , the stress range histogram $\Delta\sigma_i$, $i\in(1,n)$ is determined in such a way that the design damage $D_d=1$ using Eq. (6). For each combination, the number of cycles, n, and shape of the stress range histogram are kept equal to those determined with the WIM database so as to obtain a realistic load case. Subsequently, the reliability index, β , is determined with the first order reliability method (FORM) using Eq. (4, 5). The reliability index, β , is as follows related to the probability of failure, P_f :

$$P_f = \Phi(-\beta) \tag{7}$$

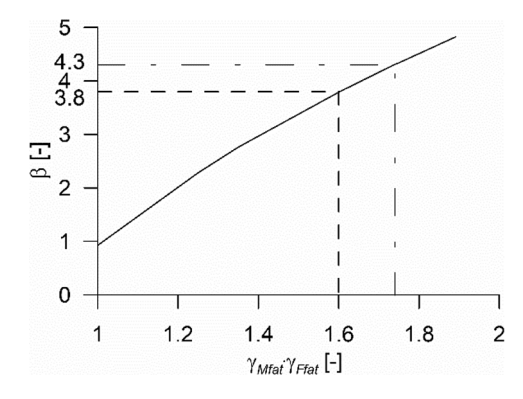


Fig. 16. Relation between combination values $\gamma_{Mfat} \cdot \gamma_{Ffat}$ and the calculated reliability index, β .

Table 4 Target values of the reliability index for a 50 reference period, β_{tar} , for a 'safe life' design depending on the reliability class (RC) and partial factor for fatigue loads, γ_{Ffat} , required to reach these values.

RC	Consequences of failure	$\beta_{tar}[-]$	γ_{Ffat} $[-]$
RC3	Large for loss of human life, or very great for economy, society or environment	4.3	1.3
RC2	Medium for loss of human life, considerable for economy, society or environment	3.8	1.2

where Φ is the cumulative distribution function of the standardised normal distribution. Crude Monte Carlo analyses were applied for a number of cases to check the FORM formulation and they showed no difference. Fig. 16 provides the relationship between the combination values γ_{Mfat} γ_{Ffat} and the calculated reliability index, β , related to a design life of 100 years.

The European standard EN 1990 [29] provides requirements with respect to the reliability of structures. For a 'safe life' design, i.e. a design not intended to be inspected, the target reliability for ultimate limit state applies. This target value depends on the resistance class (RC) and is given in Table 4 for a reference period of 50 years (columns 1–3). EN 1990 does not provide target values for a reference period of 100 years and therefore the values for 50 years are (conservatively) used here. The accompanying combination values of γ_{Mfat} · γ_{Ffat} can be read from Fig. 16 (dashed lines).

The recommended partial factor for the fatigue resistance in EN 1993–1-9 is equal to $\gamma_{Mfat}=1.35$ in case of 'large consequences of failure' and a 'safe life' design. Using Fig. 16, the values that are required for the load side are $\gamma_{Ffat}=\frac{1.74}{1.35}=1.3$ for RC3 and $\gamma_{Ffat}=\frac{1.60}{1.35}=1.2$ for RC2, see the 4th column of Table 4.

Note that the partial factors γ_{Ffat} in Table 4 are determined for the case with the same stress range histogram in the design as in the probabilistic analysis. This reflects the case of a fully accurate FLM. In practice, the required factors in Table 4 can be obtained by a combination of conservatisms in the FLM-s and the partial factor. The recommended value of the partial factor γ_{Ffat} is equal to 1.0 in the Eurocodes. This implies that the factors 1.2 and 1.3 that are required to

meet the target reliability indices, must be fully obtained through conservatisms in the FLM-s. The factors are therefore indicated with dashed black lines in Fig. 13 and Fig. 14. It is clear that none of the FLM-s meet the required reliability for all influence lines considered. The average ratios $\frac{W_{el,FLM}}{W_{el,WIM}}$ of all influence lines loaded by a slow lane only for FLM 3 and 4 are 1.2 and 1.3, respectively, hence relatively close to the required values. However, the variation in this factor between the influence lines is large and the ratios are smaller in case of loading by multiple lanes. The FLM-s require either an increase of γ_{Ffat} or an increase of the specified loads in order to meet the required reliability for all cases. A far better option, however, is improving the FLM-s so that the scatter of the ratio $\frac{W_{el,FLM}}{W_{el,WIM}}$ reduces.

7. New fatigue load model

A new FLM is provided here with improved accuracy as compared to FLM3 and 4. Because of its ease in use, FLM3 is most frequently used in Europe and it is therefore taken as a basis for the new FLM. FLM3 consists of two equal lorries that cross the influence line. The resulting stress ranges are multiplied with damage equivalent factors, see the appendix. The author distinguished three main reasons for the lack of agreement between FLM3 and the actual traffic (WIM database):

- The combination of vehicle weight and axle weights in FLM3 is not realistic. A proper model contains a combination of realistic vehicle weight, axle weight and weight of a group of axles that are closely spaced;
- The calibration factor λ₁ (see the appendix) does not realistically capture the influence of the span length;
- The probability that vehicles in different lanes are located near the maximum absolute values of the influence lines, increases with increasing span. In addition, if the influence line consists of multiple peaks, the probability of different peaks being loaded simultaneously by adjacent vehicles increases with increasing span. These aspects are not considered in FLM3.

These points were considered in deriving the new FLM, as follows. The four-axis load model FLM3 in EN 1991–2 is replaced by a 5-axle

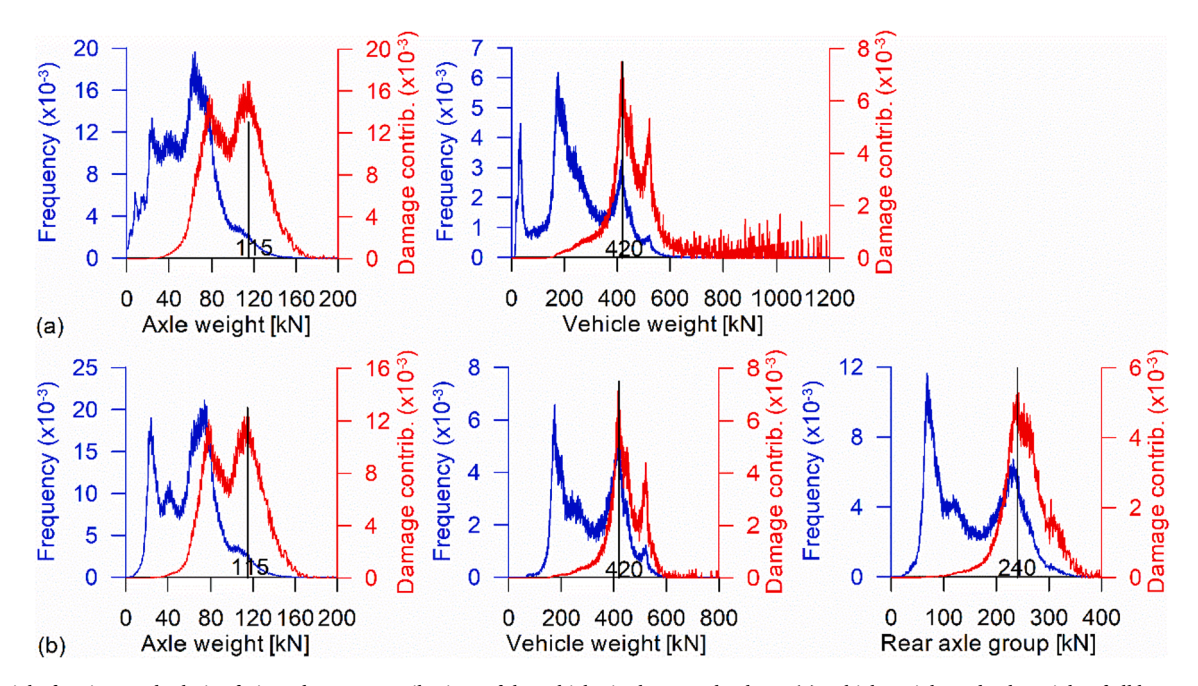


Fig. 17. Weight fractions and relative fatigue damage contributions of the vehicles in the WIM database: (a) Vehicle weight and axle weight of all heavy vehicles; (b) Vehicle weight, axle weight and weight of rear axle group of the "European lorry" group.

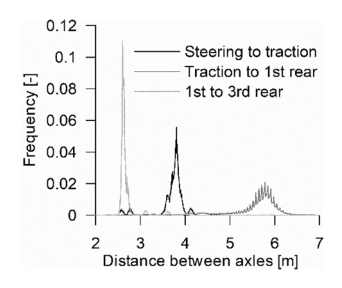


Fig. 18. Distributions of the axle distances of the "European lorry" group in the WIM database.

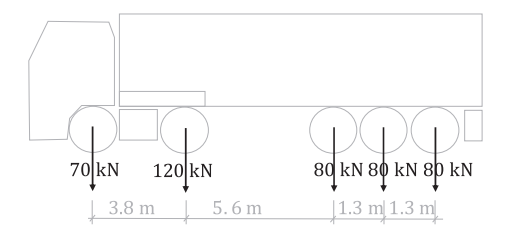


Fig. 19. Lorry comprising the new FLM.

vehicle with "European lorry" configuration according to the top graphic of Fig. 3(a), because it is the most frequently observed vehicle on European motorways, it gives the largest contribution to the fatigue damage of all vehicle types, and because it contains individual axles and a group of axles closely spaced together. For deriving the axle weights of this vehicle, the vehicle weight, axle weight and axle group weight are determined that provide the largest contribution to the fatigue damage. As a simplification, instead of considering a certain influence line, it is assumed here that each vehicle, axle, or axle group, provides one stress range, which is proportional to its weight. For a design life of 100 years, Fig. 17 provides the weight distributions of the vehicles, axles, or group of axles of the "European lorry" group in blue, left-hand vertical axis, and their relative contribution to the damage in red, right-hand vertical axis if the structure is utilized for a life of 100 years. The figure demonstrates that the large group of light weight lorries and axles do not induce fatigue damage. The relatively heavy vehicles (420 kN), axles (115 kN), and axle groups (240 kN divided over three axles), give the largest contribution to the damage. Note that these vehicles comprise a small fraction of the total volume, see Fig. 2(a) and (b). Fig. 18 provides the distances between the axles of the "European lorry" group. The figure shows that the axle distances are narrowly distributed. Based on this study, the axle weights and distances of the vehicle for the new FLM are selected, see Fig. 19.

The stress ranges, $\Delta\sigma_l$, should be determined from the crossing of this vehicle over the influence line using a rainflow or reservoir counting method as defined in the Eurocodes, implying that the stress history should be cut at the highest (or lowest) peak value and the part of the history before that peak should be transferred to the end of the history, giving a signal from peak to peak where only full ranges and no semi ranges result. These stress ranges are used to derive one equivalent range:

$$\Delta \sigma_{FLM}^* = \begin{cases} \Delta \sigma_1 & \text{if } n_l = 1\\ \left[\Delta \sigma_1^5 + \left(1 + a \frac{L}{[m]}\right) \sum_{l=2}^{n_l} \Delta \sigma_l^5 \right]^{1/5} & \text{if } n_l > 1 \end{cases}$$
(8)

where

 n_l = number of cycles encountered by crossing the vehicle over the influence line.

 $\Delta\sigma_1=$ largest stress range encountered by crossing the vehicle over the influence line.

 $\Delta \sigma_l$, $l \in (2, n_l) = \text{all}$ other stress ranges encountered by the same crossing, i.e. $\Delta \sigma_l < \Delta \sigma_1$.

L= span in case of a single span bridge, or average of the adjacent spans in case of a multi-span bridge (note: m is the distance unit of meter).

a = factor depending on the density of traffic, i.e. the number of heavy vehicles passing the bridge per unit time. Its value must be calibrated with WIM data and is given below for the database considered.

The asterisk symbol indicates that the stress range or factor is modified in comparison to FLM3. The part $(1+aL/[\mathrm{m}])$ in Eq. (8) accounts for the probability that multiple parts of the influence lines are loaded simultaneously by different vehicles. This probability increases with span L. The factors 5 and 1/5 in Eq. (8) origin from the second slope of the S-N curve ($m_2=5$). Note that only one vehicle is applied in the new FLM. The stress range applied in the verification is defined as the multiplication of this range $\Delta\sigma_{FLM}^{*}$ with the damage equivalent factor, j^* .

$$\Delta \sigma_{E2}^{*} = \lambda^{*} \cdot \Delta \sigma_{FLM}^{*} \tag{9}$$

The fatigue verification requires the design value of the resulting stress range $\Delta \sigma_{E2}$ to be equal to or smaller than the design value of the fatigue resistance at $2 \cdot 10^6$ cycles:

$$\Delta \sigma_{E2}^* \cdot \gamma_{Ffat} \le \Delta \sigma_C / \gamma_{Mfat}$$
 (10)

where $\Delta \sigma_C$ = fatigue resistance at 2·10⁶ cycles [MPa], following from the S-N curve. The damage equivalent factor λ^* should be obtained from:

$$\lambda^* = \lambda_1^* \cdot \lambda_2^* \cdot \lambda_3 \cdot \lambda_4^* \tag{11}$$

where:

$$\lambda_1^* = \begin{cases} b^{'} + c^{'} \left(\frac{L}{m}\right)^{d'} & \text{for bending moment at support } (12a) \\ \min \left[b + c \left(\frac{L}{m}\right)^{d}, e + f \frac{L}{m}\right] & \text{for all other influence lines } (12b) \end{cases}$$

$$\lambda_2^* = \frac{Q_{m,1}}{430 \text{kN}} \left(\frac{n_{Obs,1}}{10^6} \right)^{1/5} \tag{13}$$

$$\lambda_3 = \left(\frac{t_{ld}}{100 \text{ year}}\right)^{1/5} \tag{14}$$

$$\lambda_4^* = \left[1 + \left(1 + a \frac{L}{[m]} \right) \sum k = 2^{\frac{n_k}{n_{Obs,k}}} \frac{n_{Obs,k}}{n_{Obs,1}} \left(\frac{|\eta_k| \cdot Q_{m,k}}{|\eta_1| \cdot Q_{m,1}} \right)^5 \right]^{1/5}$$
(15)

$$Q_{m,k} = \left(\frac{\sum_{j=1}^{n_{Obs,k}} Q_{j,k}^{5}}{n_{Obs,k}}\right)^{1/5}$$
(16)

and:

 $t_{ld} = design life of the bridge.$

 $Q_{m,k}$ = weighted average gross vehicle weight of the heavy vehicles in lane k.

 $n_{Obs,k}$ = annual number of heavy vehicles in lane k.

 $Q_{j,k}, j \in (1, n_{Obs,k})$ = weight in kN of lorry j in lane k.

 $\eta_k=$ value of the influence line for the internal force that produces the stress range in lane k.

 $a \cdot \cdot \cdot f$ = calibration factors.

Note: k=1 is the lane for which $\Delta \sigma_{FLM}^*$ is determined. The effects of the other lanes are considered through λ_4^* , making the procedure indifferent to the choice of lane numbering and the lane at which $\Delta \sigma_{FLM}^*$ is evaluated.

Factor λ_2^* equals 0.99 for the slow lanes of the WIM database

Table 5Calibration coefficients in the new FLM.

Eq.	а	<i>b,b',b''</i>	c,c',c''	d,d'	e,e''	f,f''
(12a)	0.043	-34.	35.	0.0080	-	-
(12b)	0.043	2.2	0.0013	1.12	1.4	0.067
(18)	0.043	1.5	0.066	-	2.3	0.0035

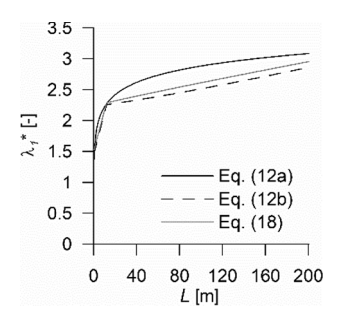


Fig. 20. Factors λ_1^* in the new FLM.

considered and the ratio $\frac{n_{Obs,2}}{n_{Obs,1}} \left(\frac{Q_{m2}}{Q_{m1}} \right)^3 = 0.11$ when index 1 and 2 refer to a slow and a fast lane, respectively. The calibration factors $a \cdots f$ are determined using an optimization algorithm, where the root mean square rms of the difference in elastic section modulus required for the

WIM database and for the FLM over all influence lines considered in the study, is minimized:

$$rms = \sqrt{\sum \left(\frac{W_{el,FLM} - W_{el,WIM}}{W_{el,WIM}}\right)^2} \tag{17}$$

Rows (12a) and (12b) of Table 5 gives the calibration factors where a distinguish is made between a bending moment influence line at an intermediate support, and all other influence lines. The resulting factor λ_1^{-1} is visualised in Fig. 20. Fig. 21 provides a comparison between Wel designed using this new model, and W_{el} designed with the WIM database. These results are produced with an S-N curve including cut-off, see the bottom graph of Fig. 11(a). Additional simulations have been carried out with an S-N curve without cut-off (centre graph of Fig. 11(a)) and an S-N curve with slope parameter $m_1 = 5$, the latter being relevant for shear loaded welded joints. Table 6 lists the mean value and standard deviation of the ratio $\frac{W_{el,HM}}{W_{el,WM}}$ for all cases. Note that the new model is calibrated for a mean ratio of 1. The load effect must be multiplied by the partial factors γ_{Ffat} of Table 4 in order to take account of the load uncertainties. Fig. 21 and the standard deviation in Table 6 indicate that the model is much more accurate than FLM3 and 4, whereas it has approximately the same ease of use for practitioners as FLM3 and is easier to use than FLM4.

For any other WIM database, the simulations with the different influence lines and spans as considered in Fig. $21\,$ can be repeated and

 $W_{el WIM}$ determined for each simulation. Standard solving algorithms available in commercial software, such as the GRG nonlinear solver of MS Excel or the optimoptions algorithm of Mathlab, can be adopted to minimize the *rms* of Eq. (17) by changing calibration coefficients a to f. To study the tolerance of the procedure, it is applied to two other WIM databases with different characteristics than the A16 database. The first one is a one-week database recorded at one lane in motorway E6 near Löddeköpinge, Sweden, in 2009. The number of vehicles per week is 31% of that of the A16 database and it contains a larger fraction of vehicles weighing more than 500 kN, but a smaller fraction of axles weighing more than 100 kN. The second database is a one-year database recorded in motorway 1 near Denges, Switzerland, in 2017. The number of vehicles per week is 19% of that of the A16 database, it contains smaller fractions of heavy vehicles and axles, it contains a much larger fraction of two-axle vehicles and it contains a large fraction of vehicles on the fast lanes. Applying the new FLM gives a good match for the Swedish database with calibration factors as in Table 5, whereas the Swiss database requires recalibration coefficients a to f because of the different vehicle characteristics. After recalibration, the standard deviations of the ratio $\frac{W_{el,FLM}}{W_{el,WDM}}$ as defined in Table 6 are 0.04 and 0.05 for the Swedish and Swiss databases, respectively (average equal to 1 for both databases). The low standard deviations demonstrate the general applicability of the proposed procedure.

Because $\Delta\sigma_{FLM}^*$ in Eq. (8) takes account of the possibility of multiple peaks in the influence line, the difference in λ_1^* between a bending moment influence line at an intermediate support (Eq. (12a)) and all other influence lines (Eq. (12b)) is smaller as compared to the difference between 'midspan' and 'support' in FLM3, as is demonstrated in Fig. 20. The remaining difference is attributed to the curved, wide peaks in the influence lines of type (12a) versus the sharp, narrower peaks in the influence lines of type (12b). Part of this remaining difference is unavoidable for load models based on one vehicle only. A difference in λ_1^*

Table 6 Standard deviation (and mean value) of the ratio $\frac{W_{el,FLM}}{W_{el,WIM}}$ for a design life of 100 years, for all influence lines loaded by a slow lane.

S-N curve	FLM3 a)	FLM4 b)	New FLM factors of Table 5 b)	New FLM factors recalibrated ^{b)}
$m_1 = 3$, with cut-off	0.21 (1.19)	0.17 (1.27)	0.04 (1.00)	
$m_1 = 3$, without cut- off	0.19 (1.09)	0.13 (1.30)	0.05 (0.94)	0.05 (1.00)
$m_1 = 5$, without cut- off	0.21 (1.22)	0.17 (1.27)	0.05 (1.05)	0.04 (1.00)

^{a)} Only considering results for spans between 1 m and 80 m span.

b) Spans between 1 m and 200 m.

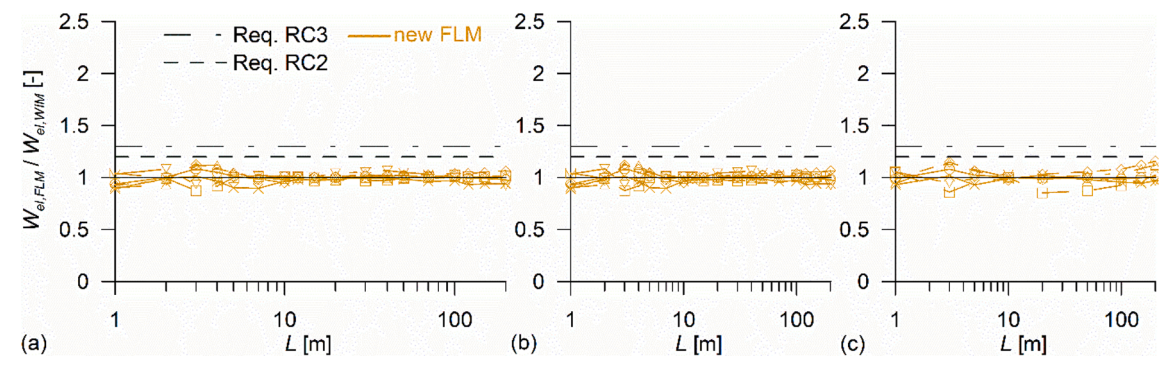
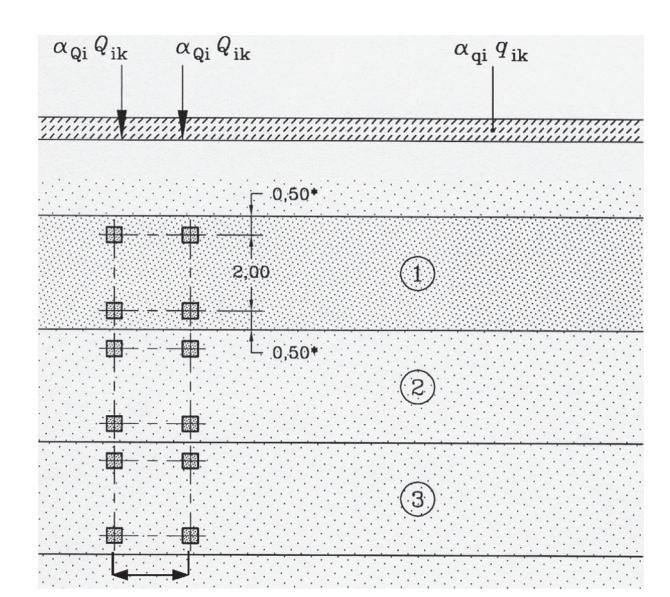


Fig. 21. Ratios Welinum of the new FLM: (a) Single slow lane; (b) Slow and fast lanes, 1 direction; (c) Slow and fast lanes, 2 directions.



Location	$lpha_{Qi}Q_{ik}$	$lpha_{qi}q_{ik}$
Lane no. 1	210 kN	2.7 kN/m ²
Lane no. 2	140 kN	0.75 kN/m ²
Lane no. 3	70 kN	0.75 kN/m ²
Other lanes	0 kN	0.75 kN/m ²
Remaining	0 kN	0.75 kN/m ²
area		

Fig. 22. Configuration and load values of FLM1 (distances in m).

between the two types of influence line implies a discontinuity when shifting from midspan to support. For this reason, an alternative, simplified fit is made that covers all influence lines considered, where Eq. (12) is replaced by:

$$\lambda_1^* = \min\left(b^{"} + c^{"} \frac{L}{m}, e^{"} + f^{"} \frac{L}{m}\right)$$
 (18)

The fit factors are provided in Table 5 and λ_1^* is plot in Fig. 20. Obviously, this simplified and generic fit provides a reduced accuracy. The standard deviation of the ratio $\frac{W_{el,FlM}}{W_{el,WlM}}$ when using Eq. (18) is 0.07 (with average value of 1.00). The performance is thus still much better as compared to FLM3 and 4, Table 6.

8. Conclusions

Traffic data measured with a WIM station offer a good basis for deriving fatigue load models (FLM-s) for road bridges. The accuracy of such a database can be cross-checked with strain gauge measurements on a structure. Based on such a cross-check, the WIM database used in this paper appears to be accurate, with a deviation of a few percent maximum in the damage. This paper demonstrates that a WIM database can be used directly for fatigue verifications instead of using random simulations with vehicle weight distributions based measurements. This has advantages because of the difficulties in simulating overtaking vehicles, traffic jams and very heavy vehicle types with low frequencies. Two methods are provided that can be used to evaluate the size of the WIM database required for an accurate representation of the fatigue load. The first method consists of composing the damage over a longer period from distributions of the damage generated per day. The second method consists of randomly selecting vehicles in the WIM database using the bootstrap method, thereby maintaining the intervehicle distances. A database size of one month or 2·105 heavy vehicles is more than sufficient for a representative fatigue verification: the calculated variation in damage between months (without considering trends or economic developments) is in the order of 1%.

Comparing different WIM databases within Europe reveals that the vehicle loads can differ between different trajectories or countries. The current FLM-s in the European standard EN 1991-2 are based on the traffic near Auxerre measured in 1986 and it appears that this traffic is still relatively heavy as compared to the majority of recent WIM databases. In addition to different weights, differences in the intervehicle distances occur between the WIM databases and this also influences the

load effects relevant to fatigue. In agreement with other studies, this paper concludes that the most used FLM no. 3 in the standard is inaccurate – for some influence lines underpredicting and for others overpredicting the actual load effect – and should be updated. In addition, this paper concludes that the other FLM-s in EN 1991-2 are also inaccurate.

Because of the differences in traffic between trajectories and countries, it may be necessary to derive load models for different groups of motorways. To do so, this paper provides a method that allows for a more accurate calibration of FLM-s than the current state of the art. It consists of selecting a single vehicle that represents the vehicle weight, axle weight and axle group weight that give the largest contributions to the fatigue damage and subsequently multiply it with damage equivalent factors. These factors contain constants that can be optimized using an automized algorithm as to provide the correct load effect. Using this procedure, the standard deviation of the resulting elastic section modulus designed with a FLM as compared to those required according to the WIM database can be reduced from 0.17 to 0.21 as observed for the current FLM-s, to 0.04 with the new FLM. The new FLM can be used for single or multiple span influence lines with spans ranging between 1 and 200 m.

Declaration of Competing Interest

The author declared that there is no conflict of interest.

Table 7Lorries constituting FLM2 (first axle is steering axle, last axle is rear axle).

Lorry	No. axles	Axles spacing [m]	Axles weight [kN]
1	2	4.5	90, 190
2	3	4.2, 1.3	80, 140, 140
3	5	3.2, 5.2, 1.3, 1.3	90, 180, 120, 120, 120
4	4	3.4, 6.0, 1.8	90, 190, 140, 140
5	5	4.8, 3.6, 4.4, 1.3	90, 180, 120, 110, 110

Table 8
Lorries constituting FLM4 (first axle is steering axle, last axle is rear axle).

raction of N _{Obs,1}
.20
.05
.50
.15
.10

Acknowledgements

The Dutch road bridge asset owner Rijkswaterstaat is acknowledged for providing the WIM database and for permission to publish the database results and the strain gauge measurements. Alain Nussbaumer (EPFL) is acknowledged for the discussions related to the influence of traffic jams. The company Movares is acknowledged for producing the influence lines of Fig. 4b.

Appendix. . Description of the FLM-s in EN 1991-2

The text in this annex is taken as close as possible to EN 1991-2, but sometimes modified to enhance readability.

Fatigue load model 1

FLM 1 consists of double-axle concentrated loads $\alpha_{Qi}Q_{ik}$ and uniformly distributed loads $\alpha_{qi}q_{ik}$ applied on notional lanes, with the values of the loads indicated in Fig. 22. The bridge is divided into notional lanes with a width of (usually) 3 m. As many notional lanes as possible between kerbs or between the inner limits of vehicle restraint systems should be applied. The notional lane giving the most unfavourable effect is numbered Lane Number 1, the lane giving the second most unfavourable effect is numbered Lane Number 2, etc. The maximum and minimum stresses ($\sigma_{FLM,max}$ and $\sigma_{FLM,min}$) should be determined from all possible load arrangements of the model on the bridge. The design value of the resulting stress range $\Delta\sigma_{FLM1} = \sigma_{FLM1,max} - \sigma_{FLM1,min}$ should be equal to or smaller than the design value of the constant amplitude fatigue limit of the applicable S-N curve:

$$\Delta \sigma_{FLM1} \cdot \gamma_{Flat} \le \Delta \sigma_D / \gamma_{Mlat}$$
 (19)

Fatigue load model 2

FLM2 is more accurate than FLM1 when the simultaneous presence of several lorries on the bridge can be neglected for fatigue verifications. If that is not the case, it should be used only if it is supplemented by additional data. FLM2 consists of a set of idealised lorries, called "frequent" lorries, given in Table 7. The maximum and minimum stresses ($\sigma_{FLM2,max}$ and $\sigma_{FLM2,min}$) should be determined from the most severe effects of different lorries, separately considered, travelling alone along the appropriate lane. The design value of the resulting stress range $\Delta \sigma_{FLM2} = \sigma_{FLM2,max} - \sigma_{FLM2,min}$ should be equal to or smaller than the design value of the constant amplitude fatigue limit of the applicable S-N curve:

$$\Delta \sigma_{FLM2} \cdot \gamma_{Flat} \le \Delta \sigma_D / \gamma_{Mfat}$$
 (20)

Fatigue load model 3

FLM3 consists of four axles, each of them having two identical wheels. The weight of each axle is equal to 120 kN and the distance between the axles is 1.2, 6.0 and 1.2 m. Where relevant, two vehicles in the same lane should be taken into account. Recommended conditions for the second vehicle are a geometry as defined for the first vehicle and the weight of each axle is equal to 36 kN (instead of 120 kN). The distance between the two vehicles, measured from centre to centre of vehicles, is not less than 40 m. The maximum and minimum stresses and the stress ranges for each cycle of stress fluctuation, $\Delta \sigma_{FLM3} = \sigma_{FLM3,max} - \sigma_{FLM3,min}$, resulting from the transit of the model along the bridge should be calculated. This load model must be combined with the following information from EN 1993–2 for steel bridges: The stress range defined above must be multiplied by the damage equivalence factor λ :

$$\Delta \sigma_{E2} = \lambda \cdot \Delta \sigma_{FLM3} \tag{21}$$

The damage equivalent λ for bending moments in road bridges up to 80 m span should be obtained from:

$$\lambda = \min(\lambda_1 \cdot \lambda_2 \cdot \lambda_3 \cdot \lambda_4, \lambda_{max}) \tag{22}$$

$$\lambda_1 = \begin{cases} 2.55 - 0.01(l_i - 10) & \text{at midspan} \\ \max[2.0 - 0.015(l_i - 10), 1.7 + 0.01(l_i - 30)] & \text{at a support} \end{cases}$$
 (23)

$$\lambda_2 = \frac{Q_{m,1}}{480 \text{kN}} \left(\frac{n_{Obs,1}}{5 \cdot 10^5} \right)^{1/5} \tag{24}$$

$$\lambda_3 = \left(\frac{t_{ld}}{100 \text{year}}\right)^{1/5} \tag{25}$$

$$\lambda_4 = \left[1 + \sum_{k=2}^{n_k} \frac{n_{Obs,k}}{n_{Obs,1}} \left(\frac{\eta_k Q_{mk}}{\eta_1 Q_{m1}} \right)^5 \right]^{1/5} \tag{26}$$

$$Q_{m,k} = \left(\frac{\sum_{j=1}^{n_{Obs,k}} Q_{j,k}^{S}}{n_{Obs,k}}\right)^{1/5} \tag{27}$$

$$\lambda_{max} = \begin{cases} \max[2.0, 2.5 - 0.033(l - 10)] & \text{at midspan} \\ \max[1.8, 1.8 + 0.018(l - 30)] & \text{at a support} \end{cases}$$
 (28)

where:

 l_i = span for bending moment or shear at mispan, average of the adjacent spans for bending moment at intermediate supports, and 0.4 times the span for shear at a support.

 Q_{mk} = weighted average gross vehicle weight (kN) of the heavy vehicles in lane k.

 $n_{Obs,k}$ = number of heavy vehicles in lane k.

 $Q_{j,k}, j \in (1, n_{Obs,k})$ = weight in kN of lorry j in lane k.

 η_k = value of the influence line for the internal force that produces the stress range in the

centre of lane k, to be inserted in Eq. (26) with positive sign.

For the WIM database of motorway A16, $\lambda_2=1.017$ when considering all vehicles with a weight exceeding 35 kN on the slow lane. The value for λ_2 does not change if the weight limit is increased to 150 kN, demonstrating that the value is insensitive to the definition of a heavy vehicle. The ratio

 $\frac{n_{Obs,2}}{Q_{omi}} \left(\frac{Q_{m2}}{Q_{omi}} \right)^5$ for the WIM database equals 0.11 if lane 2 is the fast lane. The design value of the resulting stress range $\Delta \sigma_{E2}$ should be equal to or smaller

than the design value of the fatigue resistance at $2^{\cdot}10^{6}$ cycles:

$$\Delta \sigma_{E2} \cdot \gamma_{Ffat} \le \Delta \sigma_C / \gamma_{Mfat}$$
 (29)

Fatigue load model 4

FLM4 consists of sets of standard lorries as defined in Table 8 for long distance traffic. The annual number of heavy vehicles, $N_{Obs,1}$, is fixed at 2 million for motorway bridges. This model simulates traffic which is deemed to produce fatigue damage equivalent to that due to actual traffic. Each standard lorry is considered to cross the bridge in the absence of any other vehicle, however, many national annexes prescribe that 10% of the vehicles on the slow lane must be applied simultaneously with a vehicle on the adjacent lane. This addition is incorporated in the comparison of the main document. The stress range histogram should be determined using the rainflow or reservoir counting methods from each fluctuation in stress during the passage of the lorries on the bridge. This histogram contains all stress cycles $\Delta \sigma_i$. The fatigue damage, D, should be determined using Eq. (6) of the main body of this paper. The design damage should be equal to or smaller than 1.

References

- [1] EN 1991-2, Eurocode 1: Actions on structures Part 2: Traffic loads on bridges. CEN, Brussels, 2003.
- [2] Bruls A, Croce P, Sanpaolesi L, Sedlacek G, ENV 1991 Part 3: traffic loads on bridges - calibration of road load models for road bridges, IABSE colloquium: basis of design and actions on structures, Delft, vol. 74, 1996, pp. 77–84.
- [3] Bruls A, Calgaro M, Mathieu, Prat M: ENV 1993 Part 3: The main model of traffic loads on road bridges – Background studies, Proceedings of IABSE colloquium on the basis of design and actions on structures, Delft, vol. 74, 1996.
- [4] Croce P. Background to fatigue load models for Eurocode 1: part 2 traffic loads. Prog Struct Eng Mater 2001;3:335–45.
- [5] Sedlacek G, Merzenich G, Paschen M, et al. Background document to EN 1991: part 2 - traffic loads for road bridges and consequences for the design. JRC Scientific Technical Rep 2008.
- [6] Lehrke Steinhilber. Buxbaum: Erweiterte Auswertung von Verkehrslastmessungen im Hinblick auf die Generierung eines Verkehrsbildes aus statischen Kennwerten, Frauenhofer-Institut für Betriebsfestigkeit, Darmstadt. Bericht 1988;6227.
- [7] Seifert: Fatigue loading and design for road bridges, Dissertation TH Darmstadt (1989).
- [8] Jacob B, O'Brien E, Jehaes S. Weigh in motion of road vehicles. Cost 323 final report (1993-1998) Appendix 1 European WIM specification. Laboratoire Central des Ponts et Chaussées, Paris, 2002.
- [9] Meystre T, Hirt MA. Evaluation de ponts routiers existants avec un modèle de charges de trafic actualisé. Mandat de recherche AGB2002/005, Office Fédéral des Routes, OFROU, Publication VSS594, Bern, 2006.
- [10] Maddah N, Nussbaumer A. Analytical approach for improving damage equivalence factors. Eng Struct 2014;59:838–47.
- [11] Maddah N, Nussbaumer A. Evaluation of Eurocode damage equivalent factor based on traffic simulation. Proceedings of the sixth international IABMAS conference 2010/04/15 (2010).
- [12] Croce P. Impact of road traffic tendency in europe on fatigue assessment of bridges. Appl. Sci. 2020;10:1389. https://doi.org/10.3390/app10041389.
- [13] Chatzis M, Tirkkonen T, Lilja H. Calibrating Eurocode's fatigue load model 3 to specific national traffic composition. Struct. Eng. Int. 2012;22:232–7.
- [14] Leander J. Reliability evaluation of the Eurocode model for fatigue assessment of steel bridges. J Constr Steel Res 2018;2018(141):1–8.
- [15] Nussbaumer A, Oliveira Pedro J, Baptista CA, Duval M. Fatigue damage factor calibration for long-span cable-stayed bridge decks. Porto: Proc. Colloquium ICMFM XIX: 2018.
- [16] Bianchi G. European traffic on road bridges and recalibration of damage equivalence factor for fatigue verification, Master Thesis, EPFL & IST Lisbon, June 2010
- [17] Croce P, Salvatore W. Stochastic model for multilane traffic effects on bridges. J Bridge Eng 2001;6:136–42.

- [18] Maddah N. Fatigue Life Assessment of Roadway Bridges based on Actual Traffic Loads. PhD dissertation at EPFL, Lausanne, 2013.
- [19] Caramelli S, Croce P. Influence of heavy traffic trend on EC1-2 load models for road bridges. In: Clemente P, De Stefano A, editors. WIM (Weigh In Motion). Roma: Load Capacity and Bridge Performance. ENEA; 2010. p. 157–64.
- [20] EN 1993-1-9, Eurocode 3: Design of steel structures Part 1-9: Fatigue, CEN, 2006.
- [21] Nussbaumer A, Borges L, Davaine L. Fatigue design of steel and composite structures. 2nd Ed. Berlin: Wiley; 2018.
- [22] Allaix DG. Bridge Reliability Analysis with an Up-to-Date Traffic Load Model. Politecnico di Torino 2007.
- [23] Nowak M, Straub D, Fischer O. Statistical Extrapolation for Extreme Traffic Load Effect Estimation on Bridges. In: Caspeele R, editor. 14th International Probabilistic Workshop. Springer International Publishing AG; 2017. p. 13–53.
- [24] JCSS probabilistic model code, https://www.jcss.byg.dtu.dk/Publications/ Probabilistic Model Code. See also: Vrouwenvelder, ACWM. The JCSS probabilistic model code. Struct Saf 1997;19:245-51.
- [25] Caprani CC, González A, Paraic R, O'Brien EJ. Assessment dynamic ratio for traffic loading on highway bridges. Struct Infrastruct Engn 2011;8:295–304.
- [26] Brady SP, O'Brien EJ, Žnidarič A. The effect of vehicle velocity on the dynamic amplification of a vehicle crossing a simply supported bridge. J Bridge Engn 2006; 11:241.0
- [27] Drebenstedt K, Euler M. Statistical Analysis of Fatigue Test Data according to Eurocode 3. In: Maintenance, Safety, Risk, Management and Life-Cycle Performance of Bridges – Powers, Frangopol, Al-Mahaidi & Caprani (Eds) Taylor & Francis Group, London, 2018, pp 2244–51.
- [28] DNVGL-RP-C210. Probabilistic methods for planning of inspection for fatigue cracks in offshore structures. DNVGL, Oslo, 2019.
- [29] EN 1990 Eurocode: Basis of design. CEN, Brussels, 2002.
- [30] Bathias C. There is no infinite fatigue life in metallic materials. Fatigue Fract Eng Mater Struct 1999;22:559–65.
- [31] Pyttel B, Schwerdt D, Berger C. Very high cycle fatigue is there a fatigue limit? Int J Fatigue 2011;33:49–58.
- [32] Kühn B, Lukić M, Nussbaumer A, et al. Assessment of Existing Steel Structures: Recommendations for Estimation of Remaining Fatigue Life. JRC-ECCS report EUR 23252 EN – 2008.
- [33] Fisher JW, Nussbaumer AC, Keating PB, Yen BT. Resistance of Welded Details under Variable Amplitude Long-Life Fatigue Testing. National Cooperative Highway Research Program (NCHRP) Report 354, Highway Research Board, Washington, D.C., 1993.
- [34] Schilling C. Fatigue of welded steel bridge members under variable amplitude loadings, NCHRP report (188).
- [35] Fisher JW. Resistance of welded details under variable amplitude long-life fatigue loading, Vol. 354, Transportation Research Board, 1993.
- [36] Leonetti D, Maljaars J, Snijder HH. Fitting fatigue test data with a novel S-N curve using frequentist and Bayesian inference. Int J Fatigue 2017;105:128–43.